Journal of proteome research

Article

pubs.acs.org/jpr

Detection of Dichlorvos Adducts in a Hepatocyte Cell Line

Tri M. Bui-Nguyen,[†] William E. Dennis,[‡] David A. Jackson,[‡] Jonathan D. Stallings,[‡] and John A. Lewis*[,‡]

[†]Oak Ridge Institute for Science and Education (ORISE) Postdoctoral Researcher, U.S. Army Center for Environmental Health Research, 568 Doughten Drive, Fort Detrick, Maryland 21702, United States

[‡]U.S. Army Center for Environmental Health Research, 568 Doughten Drive, Fort Detrick, Maryland 21702, United States

Supporting Information

ABSTRACT: The toxicity of dichlorvos (DDVP), an organophosphate (OP) pesticide, classically results from modification of the serine in the active sites of cholinesterases. However, DDVP also forms adducts on unrelated targets such as transferrin and albumin, suggesting that DDVP could cause perturbations in cellular processes by modifying noncholinesterase targets. Here we identify novel DDVP-modified targets in lysed human hepatocyte-like cells (HepaRG) using a direct liquid chromatography−mass spectrometry (LC−MS) assay of cell lysates incubated with DDVP or using a competitive pull-down experiments with a biotin-linked organophosphorus compound (10-fluoroethoxyphosphinyl-*N*-biotinamidopentyldecanamide; FP-biotin), which competes with DDVP for similar binding sites. We show that DDVP forms adducts to several proteins important for the cellular metabolic pathways and differentiation, including glyceraldehyde-3-phosphate dehydrogenase (GAPDH) and actin. We validated the results using purified proteins and enzymatic assays. The study not only identified novel DDVP-modified targets but also suggested that the modification directly inhibits the enzymes. The current approach provides information for future hypothesis-based studies to understand the underlying mechanism of toxicity of DDVP in non-neuronal tissues. The MS data have been deposited to the ProteomeXchange with identifier PXD001107.

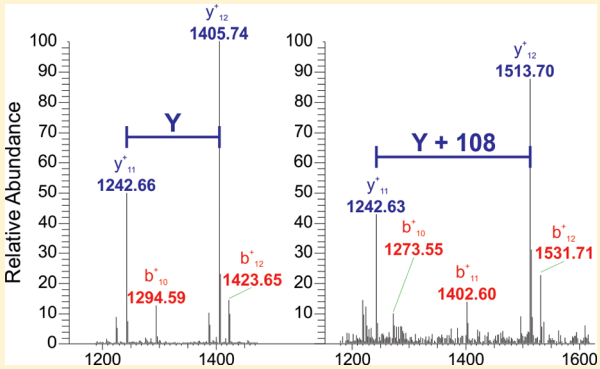

KEYWORDS: *dichlorvos, HepaRG, protein adduct, organophosphate pesticide*

INTRODUCTION

Organophosphorus (OP) agents have been widely used to control disease vectors worldwide. Dichlorvos (DDVP), an organophosphate, was once among the most popular commercially available pesticides and was used mainly indoors for insect and parasite control in livestock.[1] Despite its acute and chronic toxicity,[2−4] DDVP remains commercially available. DDVP is well known for its effects on the parasympathetic autonomic nervous system[5] and the neuromuscular systems.[3] Recent studies also suggest that DDVP affects non-neuronal targets in human plasma,[6] the liver,[7−9] the kidney,[10] and the reproductive system.[11,12] In the liver, the primary site of DDVP metabolism,[7−9] DDVP has been shown to induce hepatocellular vacuoles and cell swelling.[13]

DDVP is rapidly and efficiently metabolized[7] to desmethyldichlorvos, dimethyl phosphate, and dichloroacetaldehyde (DCA) by a glutathione-dependent pathway and by the aryl esterase pathway without accumulating in the tissues.[8,9,14] The quickness and efficiency of DDVP metabolism have hitherto presented challenges in identifying the molecular targets or adducts of DDVP in liver tissues.

The formation of an adduct on the active site serine of acetylcholinesterase accounts for the primary toxicity of DDVP by inhibition of acetylcholinesterase and accumulation of acetylcholine at the synaptic cleft.[15] Past work has looked for adducts on non-neuronal targets that may contribute to the toxicity of OP using pure isolated proteins.[16−18] OP-modified proteins in different biological matrixes have been identified by either directly analyzing purified proteins incubated with the OP of interest or by utilizing the biotin-linked organophosphorus compound 10-fluoroethoxyphosphinyl-*N*-biotinamidopentyldecanamide (FP-biotin) in a competitive-pull down assay.[18,19] Hitherto, using these strategies, approximately a dozen proteins have been shown to form adducts to DDVP.[16,20−22]

Two distinct DDVP adducts are formed by covalent bonding to the hydroxyl group of tyrosine, serine, and threonine residues.[20] A dimethyl phosphate adduct results from the loss of the dichlorovinyl group upon the formation of the initial covalent bond with the protein. Through a secondary process termed "aging," this adduct is dealkylated by losing a methyl group to create the second form, methyl phosphate. The masses of the unaged and aged adducts are 108 and 94 amu, respectively. Because the aged adduct is resistant to oxime

Received: January 2, 2014
Published: June 30, 2014

   dx.doi.org/10.1021/pr5000076 | *J. Proteome Res.* 2014, 13, 3583−3595

treatments,[23] the rate of aging is an important consideration when determining toxicity of different OP compounds.

In the present study, we used two mass spectrometry strategies with cell lysates to identify a population of proteins forming adducts with DDVP (Figure 1A). We first incubated

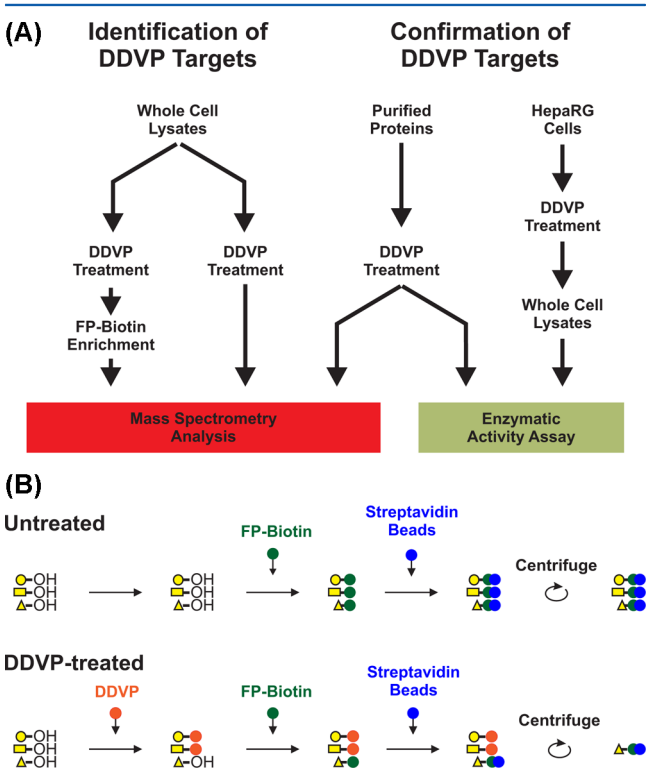

Figure 1. (A) Multipronged workflow used in this study is diagramed. Targets of DDVP adduct formation were identified by incubating cell lysates with DDVP and analyzing the proteins by LC–MS/MS; either directly or following an FP-biotin enrichment strategy. Confirmation of a subset of the targets was performed via LC–MS/MS on purified proteins after incubation with DDVP or via enzymatic activity assays on purified proteins and whole cells after exposure to DDVP. (B) FP-biotin enrichment is a competitive assay in which pretreatment of proteins with DDVP blocks the FP-biotin bonding site. A reduction in protein abundance in enriched samples after incubation with DDVP provides indirect evidence of DDVP adduct formation.

lysates of a human hepatocyte-like cell line (HepaRG) with DDVP. Then, we identified DDVP-modified targets in these lysates either with shotgun proteomics or with a pull-down assay using FP-Biotin, which competes with DDVP for similar binding sites (Figure 1B). We validated the results for a subset of the targets using pure isolated proteins with mass spectrometry and enzymatic assays. Finally, we performed quantitative proteomics on exposed cells to examine the relationship between DDVP-formed adducts and DDVP-induced acute proteomic changes.

MATERIALS AND METHODS

Cell Lysates and DDVP Exposure

HepaRG cells, culture media, and supplements were obtained from Life Technologies (Carlsbad, CA). HepaRG cells are terminally differentiated hepatic cells derived from a human hepatic progenitor cell line. Cells were cultured as per the manufacturing protocols. Whole cell lysates were generated by probe sonication in lysis buffer (20 mM TRIS-HCl, 5 mM $MgCl_2$, 5 mM $CaCl_2$, 1 mM DTT, and 100 mM KCl, pH 7.5) with three cycles of 15 s on and 5 s off at 20% power using a Vibra Cell sonicator (Sonics & Materials, Danbury, CT). Soluble fractions were collected by centrifugation for 20 min at 16 000 × g. Cell lysates were incubated with different concentrations of DDVP (50, 500, or 5000 μM) in binding buffer (100 mM KCl, 50 mM NH_4HCO_3, and 3% glycerol, pH 7.5) for 1 h for FP-biotin assays or 2 h for direct MS/MS assays. Two sets of incubations were performed. The first set used only a 5 mM concentration, and the second set used a range of concentrations from 0.05 to 5 mM; each set included an unexposed control. Four replicate incubations were performed for each condition except the second round of the direct MS/MS assay, which had three. See Supplemental Table 1 in the Supporting Information for a list of exposure sets. Proteome Discoverer search results from each round were combined to generate the final lists of proteins.

FP-Biotin

Cell lysates were subjected to competitive pull-down experiments using FP-biotin method as previously described with minor modifications (Figure 1B).[18,19] Standard conditions for FP-biotin-pull-down assay were as follows. Untreated lysates or DDVP-treated lysates (1 mg) were incubated with 10 μg of FP-biotin (Toronto Research, ON, Canada) in binding buffer (final volume of 1 mL) for 1 h at 37 °C. FP-biotin-bound proteins were then recovered on agarose avidin beads (Life Technologies, Grand Island, NY) as previously described.[18] Bound proteins were eluted with 1% RapiGest (Waters, Milford, MA) in 50 mM NH_4HCO_3 at 95 °C and subjected to mass spectral analysis.

Purified Proteins

Human glyceraldehyde-3-phosphate dehydrogenase from erythrocytes (GAPDH, G6019) was obtained from Sigma (St. Louis, MS), human actin gamma recombinant protein (ACTG1, H00000071) and lactate dehydrogenase A recombinant protein (LDH, H00003939) were obtained from Novus Biologicals, Littleton, CO. Purified proteins (up to 10 μg) were incubated with DDVP (5 mM) in binding buffer for 2 h. The reactions were quenched by 1% heated RapiGest in 50 mM NH_4HCO_3 at 65 °C. Treated proteins were subjected to LC–MS/MS. GAPDH was analyzed in single run. The LDH and actin samples were analyzed twice.

Chemical Analysis

DDVP concentrations were verified by analysis on a Hewlett-Packard gas chromatograph equipped with a 6890 model series auto injector. Ions were measured for DDVP with an electron capture detector. Analytical standards for DDVP and metabolites were purchased from Chem Service (West Chester, PA).

Mass Spectrometry Sample Prep and Analysis

Treated cell extracts or purified proteins were denatured in 0.1% RapiGest and 5 mM DTT at 60 °C for 30 min. Once cooled, iodacetamide (15 mM final concentration) was added, and the samples were incubated at room temperature for 30 min. Proteins were digested with a 1:50 ratio of trypsin gold (Promega, Madison, WI) to protein at 37 °C overnight. The resulting peptides were separated on a Proxeon EASY nano-LC (Thermo Scientific, Waltham, MA) using a Waters nano-Acquity UPLC column (BEH C18 100 μm × 100 mm, 1.7 μm particle size) in-line with an Orbitrap Velos mass spectrometer (Thermo Scientific). With the exception of the LDH and actin

dx.doi.org/10.1021/pr5000076 | J. Proteome Res. 2014, 13, 3583–3595

Table 1. Proteins Forming Adducts with DDVP Identified by FP-Biotin Competitive Pull-Down Assay

unique peptides	protein gi	description	select catalytic functions	direct MS/MS[a]
2	323276700	40S ribosomal protein S10		TRUE
3	4506685	40S ribosomal protein S13		
2	312284072	40S ribosomal protein S17-like		
2	11968182	40S ribosomal protein S18		
2	4506695	40S ribosomal protein S19		
2	4506697	40S ribosomal protein S20 isoform 2		
2	4506707	40S ribosomal protein S25		
4	15718687	40S ribosomal protein S3		
5	4506723	40S ribosomal protein S3a		
8	4506725	40S ribosomal protein S4, X isoform X isoform		
3	13904870	40S ribosomal protein S5		
3	14141193	40S ribosomal protein S9		
2	315221152	60S ribosomal protein L11 isoform 2		
2	4506597	60S ribosomal protein L12		
2	341604770	60S ribosomal protein L13 isoform 3		
2	4506607	60S ribosomal protein L18		
3	4506609	60S ribosomal protein L19		
2	4506605	60S ribosomal protein L23		
2	4506631	60S ribosomal protein L30		
2	14591909	60S ribosomal protein L5		
2	67944630	60S ribosomal protein L9		
2	4501867	aconitate hydratase, mitochondrial	lyase	
7	4501887	actin, cytoplasmic 2		TRUE
2	5453722	acyl-protein thioesterase 1	hydrolase	
3	71773201	adenine phosphoribosyltransferase isoform b	transferase	
4	4502209	ADP-ribosylation factor 5		
9	5453543	aldo-keto reductase family 1 member C1	aldo-keto reductase	TRUE
3	156523970	alpha-2-HS-glycoprotein preproprotein		
5	4503571	alpha-enolase isoform 1	enolase	TRUE
2	222136639	C-1-tetrahydrofolate synthase, cytoplasmic	hydrolase/oxidoreductase/ligase	
2	62912457	delta-1-pyrroline-5-carboxylate synthase isoform 2	oxidoreductase/transferase/kinase	
8	4503471	elongation factor 1-alpha 1		
4	34147630	elongation factor Tu, mitochondrial		
3	41872631	fatty acid synthase	hydrolase/ligase/oxidoreductase/transferase	
4	108773793	glucose-6-phosphate 1-dehydrogenase isoform b	oxidoreductase	
9	7669492	glyceraldehyde-3-phosphate dehydrogenase	oxidoreductase	TRUE
3	5453555	GTP-binding nuclear protein Ran	GTPase	
2	5174447	guanine nucleotide-binding protein subunit beta-2-like 1		
3	5729877	heat shock cognate 71 kDa protein isoform 1	ATPase activity	
5	4504517	heat shock protein beta-1		
3	154146191	heat shock protein HSP 90-alpha isoform 2	ATPase activity	
12	20149594	heat shock protein HSP 90-beta	ATPase activity	
3	157412270	heterogeneous nuclear ribonucleoprotein M isoform b		
3	74136883	heterogeneous nuclear ribonucleoprotein U isoform a		
2	18105048	histone H2B type 1-K		
3	4504301	histone H4		TRUE
4	28178825	isocitrate dehydrogenase [NADP], cytoplasmic	oxidoreductase	
6	28178832	isocitrate dehydrogenase [NADP], mitochondrial	oxidoreductase	
3	40354195	keratin, type I cytoskeletal 18		
7	24234699	keratin, type I cytoskeletal 19		
4	4504919	keratin, type II cytoskeletal 8		
2	260099727	L-lactate dehydrogenase A chain isoform 5	oxidoreductase	
2	4758332	long-chain-fatty-acid-CoA ligase 4 isoform 1	ligase	
9	12667788	myosin-9	ATPase activity	
4	5453790	nicotinamide *N*-methyltransferase	methyltransferase/transferase	
6	224809329	peptidyl-prolyl cis−trans isomerase FKBP5 isoform 1	isomerase	
2	4505591	peroxiredoxin-1	peroxidase	
2	21361621	phosphoglucomutase-1 isoform 1	phosphoglucomutase	
3	193083114	poly(rC)-binding protein 2 isoform g		
15	33286418	pyruvate kinase isozymes M1/M2 isoform a	pyruvate kinase	TRUE
4	332164777	pyruvate kinase isozymes M1/M2 isoform d	pyruvate kinase	

dx.doi.org/10.1021/pr5000076 | *J. Proteome Res.* 2014, 13, 3583−3595

Table 1. continued

unique peptides	protein gi	description	select catalytic functions	direct MS/MS[a]
2	256222019	ras-related protein Rab-10		
4	16933567	ras-related protein Rab-8A		
2	4502027	serum albumin preproprotein		
5	57013276	tubulin alpha-1B chain		TRUE
3	301171345	tubulin alpha-1C chain		TRUE
17	29788785	tubulin beta chain		TRUE
11	296040438	UDP-glucose 6-dehydrogenase isoform 3	oxidoreductase	

[a]Proteins also identified by direct MS/MS (Table 2).

direct MS/MS assay, technical replicates were not performed. In brief, 10 μL of sample in 0.1% formic acid was loaded. The gradient was formed using 0.1% formic acid in water (pump A) and 0.1% formic acid in acetonitrile (Pump B). The gradient profile for the 120 min runs began at 3% B and proceeded to 45% B at 90 min, 95% B at 100 min, 95% B at 115 min, and 3% B at 116 min through the end. The flow rate was 0.30 μL/min.

Parent ion scans were done in the Orbitrap using 100 000 resolution over the range of 400−1600 m/z. The top 10 peptides were selected for fragmentation, and both collision-induced dissociation (CID) and higher energy collisional dissociation (HCD) were performed on the selected peptides. CID settings were minimum signal threshold of 50 000, isolation with of 2 m/z, normalized collision energy of 35 V, default charge state of 2, activation Q of 0.25, and an activation time of 10 ms. The HCD settings were minimum signal threshold 50 000, resolution of 7500, isolation width of 2 m/z, normalized collision energy of 44 V, default charge state of 2, and an activation time of 0.1 ms. Dynamic exclusion was done with a repeat count of 1 with a repeat duration of 20 s. An exclusion list of up to 500 precursors was created, and the exclusion duration was 20 s. Exclusion was done relative to mass with a 10 ppm high and low limits.

Mass spectral data were processed using Thermo Proteome Discoverer 1.3. Peak lists were created using Proteome Discoverer's default peak finding algorithm and passed to Sequest to search against a database of all human proteins in the National Center for Biotechnology Information RefSeq database (downloaded 01/13/2012). To assess false-positive rates through downstream processing, a set of decoy sequences equal in length and number to the real sequences were generated using Waters' Protein Lynx Global Server 2.5 and included in the search database. Four potential contaminant proteins used for instrument checks (alcohol dehydrogenase, [Glu1]-fibrinopeptide, and two synthetic phosphopeptides) were added to the final list to create a list of 32 873 human proteins and 65 732 total sequences. The search parameters for Sequest were as follows. The mass tolerance values were set at 10 ppm for precursor ions and 0.8 Da for fragment ions, enzyme was set to trypsin, and the maximum number of missed cleavages was 2. Other search parameters included fixed modification on cysteine (carbamidomethyl) and variable modifications on methionine (oxidation) and on serine, tyrosine, or threonine (phosphorylation, *O*-methylphosphate, or *O*-dimethylphosphate). Only scans with ≤ 0.01 FDR as determined by Percolator were used for protein identification. Only proteins with at least two identified peptides were considered for further analysis. MS/MS of peptides with more than one S, T, or Y residue were visually inspected to identify the presence of a high-quality fragment ion (mass error < 200 mmu and intensity >10 000) that was able to resolve the location of adduct sites among the S, T, or Y residues. Protein abundances were evaluated using Progenesis LC−MS (Nonlinear Dynamics; Durham, NC) and Partek Genomic Suite (GS) software (St. Louis, MO). Proteins with a significant changes in abundance were selected with an FDR ≤ 0.05 based on a two-way ANOVA (concentration and exposed) with contrast analysis for each concentration and then further filtered using a 1.5 fold change from control. In the competitive FP-biotin pull-down experiments, proteins were considered to be targets for DDVP if their abundance in treated samples was reduced from controls. For shotgun proteomics of total lysates from treated cells, protein changes in either direction were considered. Pathway and ontology analyses were performed using Ingenuity Pathway Analysis (IPA; Redwood City, CA), MetaCore (Thomson Reuters; New York, NY), and Universal Protein Resource (www.uniprot.org). The mass spectrometry proteomics data have been deposited to the ProteomeXchange Consortium[24] via the PRIDE partner repository with the dataset identifier PXD001107.

Enzymatic Assays

Glyceraldehyde-3-phosphate dehydrogenase (GAPDH) and lactate dehydrogenase (LDH) enzyme activities were measured with commercial assay kits (GAPDH Assay Kit and LDH Assay Kit, respectively, BRSC, Buffalo, NY) per the manufacturer's instructions. In brief, HepaRG cells or pure isolated proteins (GAPDH and LDH) were treated with different concentrations of DDVP for 4 or 2 h, respectively. Non-DDVP-treated cells, GAPDH, and LDH were used as controls, and water was used as blank (n = 4). Percent enzymatic activity was calculated based on the controls without DDVP treatment. Statistical significance was tested using a Student's t test.

RESULTS AND DISCUSSION

FP-Biotin Competitive Pull-Down Assay to Identify Putative Targets of DDVP

FP-biotin has been used successfully to identify novel OP targets as either an organophosphorus agent or as a component of competitive pull-down assays.[18,25,26] We performed FP-biotin pull-down assays with HepaRG lysates that had been preincubated with 0, 50, 500, or 5000 μM DDVP. Of the 511 proteins identified by LC−MS/MS across all conditions using peptides with high confidence scores (FDR < 0.01), 70 had the abundance of at least one of their peptides reduced by at least 1.5 fold compared with control after preincubation with DDVP (FDR ≤ 0.05; Table 1). Assuming that DDVP blocked the FP-biotin binding sites, these 70 proteins are candidate DDVP targets.

Most of the DDVP bound proteins play crucial roles in cell organization and differentiation (ribosomal proteins, cytoskeleton proteins) or catalytic activity (oxidoreductase, lyase,

dx.doi.org/10.1021/pr5000076 | J. Proteome Res. 2014, 13, 3583−3595

ligase, transferase, hydrolase, and ATPase activity). In addition to bonding to well-known OP targets (i.e., members of the hydrolase family of enzymes),[17,27] DDVP also tagged non-hydrolase proteins such as actin, tubulin, and GAPDH. A limitation of this assay, as with most proteomics based assays, is that most of the identified DDVP targets are known to be abundant within the cytosol. It is likely that DDVP will form adducts with less abundant proteins. However, through this and other approaches,[17,20] identification of other OP/FP-biotin labeled peptides has proven to be a challenge.

Detection of DDVP Protein Adducts by LC–MS/MS

To identify additional DDVP targets and to confirm putative DDVP targets from the FP-biotin pull-down assays, we searched for adducted peptides directly by liquid chromatography coupled to tandem mass spectrometry (LC–MS/MS). We incubated HepaRG whole cell lysates with DDVP, performed LC–MS/MS analysis of the proteins, and analyzed the resulting data looking for modifications on tyrosine, serine, or threonine residues with a mass of 94 or 108 amu corresponding to *O*-methyl- or *O*-dimethyl-phosphate groups. We found 53 peptides with 90 adduct combinations out of the 2257 total peptides that were identified with high confidence (FDR < 0.01) and that were found in proteins with at least two identified peptides. We further refined this list to include only adduct combinations that had at least two peptide spectrum matches (PSMs). Also, for peptides with more than one S, T, or Y residue, adduct combinations were excluded if the location of the adduct site could not be definitively determined with a fragment ion within 0.2 Da mass error. The resulting 39 peptides (Table 2) have 51 adduct combinations and comprise a minimum of 32 unique proteins. In several cases, multiple variants of a peptide were found with different adducts (both the methyl and dimethyl forms), adduct sites, or even adducts at multiple sites simultaneously. For some proteins (tubulin, histone 4, phosphoglycerate kinase 1, enolase, and cofilin-1), DDVP adducts were identified at multiple tyrosine residues. Because some peptides were found in multiple protein sequences, it was not possible with this approach to distinguish which of the proteins had the adduct; hence, the total number of proteins affected may exceed 32.

For several of the adduct sites, there were multiple indications that the residue was modified, including finding both the methyl and dimethyl adduct on the same residue and finding peptides containing missed tryptic cleavages that overlapped the same residue. For example, two peptides within annexin—one with a missed cleavages (AYTNFDAER and AYTNFDAERDALNIETAIK) were identified with a dimethyl-phosphate on the second amino acid (Y). For one peptide in enolase, (YISPDQLADLYK), three variants were identified with adducts on the first, second, or both tyrosines (Figure 2), and for one peptide in aldo-keto reductase (HIDSAHLYNNEEQVGLAIR), both the aged and unaged adduct were found on the same residue (Figure 3). These types of findings provide internal verification of adduct data and suggest that the approach is successful in finding targets of DDVP.

While we looked for modifications on all tyrosine, threonine, and serine residues, the vast majority of the modifications were identified on tyrosine. Of the 60 peptide-adduct combinations (including those identified using purified GAPDH; see later), adducts were identified on only four threonine and five serine residues. Furthermore, only one of these nine (S49 of glutathione S-transferase A5) was found on a peptide that did not contain a tyrosine residue that was also identified as an adduct site. This suggests that DDVP has a higher specificity for tyrosine compared with threonine or serine.

Consistent with previously reported sequence patterns around OP tyrosine residue binding sites,[20,28] we found that all of the adducted tyrosines were within eight amino acids of an arginine or lysine. In addition, we also found that over half (24) of the modified tyrosines were within the vicinity of an amino acid with a hydroxyl group (±3).

Thirteen of the identified sites occurred at known phosphorylation sites, active proton donor sites, glutathione binding sites, or metal binding sites, suggesting the possibility that DDVP adducts could alter biological activities. The modifications of aldo-keto reductase family 1 members at three locations (T23, Y24, and Y55) in the active site of the enzyme, and of which one (Y55) is part of the catalytic tetrad and a known phosphorylation site, are likely to inhibit its enzymatic activity.[29] We were unable to resolve which family member (C1, C2, or C3) was modified, but inhibition of C1's catalysis of progesterone may lead to reproductive effects, and inhibition of C3's reduction Prostaglandin D_2 may contribute to asthma.[30,31] Both sites modified on histone H4 (Y73 and Y89) are part of a hydrophobic cluster at the dimer–tetramer interface of nucleosomes responsible for stabilizing the complex.[32] It is possible that modification of these sites may contribute to some of the observed carcinogenicity effects observed as a result of DDVP exposure.[33] Four of the five glycolytic enzymes identified in this work had adducts that have the potential to reduce enzymatic activity. Previously it has been shown that phosphorylation of the detected pyruvate kinase (PKM) adduct site (Y161) attenuates PKM activity,[34] and in this work we show that GAPDH activity is reduced by DDVP adducts (see later). In addition, the activity of enolase and triosephosphate isomerase (TPI) is reduced by hyperphosphorylation, although the regulator residues have not been identified.[35,36] The enolase adduct is on a known phosphorylation site (Y144),[37] while the TPI adduct sites have only been identified as phosphorylation sites in proteomic screens (http://www.phosphosite.org).

Detection of Adducts on Purified Protein Incubated with DDVP

We found nine proteins in common between the direct-binding study and the FP-biotin pull-down assay. However, other proteins such as GAPDH and LDH were identified as potential targets of DDVP in the FP-biotin pull-down assay but not in the direct binding assay. While some of the proteins in the FP-biotin list are potential false-positives due to experimental error or because they were purified in complex with DDVP targets, it is also possible that their absence in the direct study is the result of incomplete MS/MS coverage. A strategy to gain greater coverage when searching for protein adducts is to analyze purified candidate proteins incubated with the adduct-forming chemical.[38] By examining purified proteins, the overall MS/MS coverage should be increased and therefore so should the odds be increased of directly identifying an adduct, if it is present.

Purified actin, GAPDH, and LDH were incubated with DDVP (5 mM) and subjected to LC–MS/MS. As expected from the whole cell extract analysis, a DDVP-labeled peptide of actin (SYELPDGQVITIGNER) was identified. With ~95% MS/MS coverage, we also found DDVP adducts to GAPDH at two peptides (Table 3). The Y255 residue of GAPDH was identified four times with different adduct-peptide combina-

dx.doi.org/10.1021/pr5000076 | J. Proteome Res. 2014, 13, 3583–3595

Table 2. DDVP Adduct Sites Identified by LC−MS/MS of Whole Cell Lysates Incubate with DDVP

protein	PSM[a]	peptide sequence	adduct[b]	protein accession numbers[c]
14-3-3 protein gamma	2	yLAEVATGEKR	Y1-D	21464101
14-3-3 protein zeta/delta	7	yLAEVAAGDDKK	Y1-D	208973244
40S ribosomal protein S10	2	IAIyELLFK	Y4-D	323276700; 321117084
actin (alpha and gamma)	2	yPIEHGIITNWDDMEK	Y1-D	4501889; 4885049; 213688375; 4501881
actin (alpha, beta, and gamma)	12	sYELPDGQVITIGNER	S1-D	316659409; 4501887; 213688375; 4501885; 4501881; 4501889; 4885049; 63055057; 315570273; 134133226; 153791352
actin (alpha, beta, and gamma)	12	SyELPDGQVITIGNER	Y2-D	316659409; 4501887; 213688375; 4501885; 4501881; 4501889; 4885049; 63055057; 315570273; 134133226; 153791352
aldo-keto reductase family 1 (C1 and C2)	3	LNDGHFMPVLGFGtYAPAEVPK	T14-D	207028673; 45446745; 4503285; 5453543; 410169811; 410169807
aldo-keto reductase family 1 (C1 and C2)	3	LNDGHFMPVLGFGTyAPAEVPK	Y15-D	207028673; 45446745; 4503285; 5453543; 410169811; 410169807
aldo-keto reductase family 1 (C1, C2, and C3)	27	HIDSAHLyNNEEQVGLAIR	Y8-D	359806998; 359806990; 24497583; 5453543; 410169811; 410169807
aldo-keto reductase family 1 (C1, C2, and C3)	11	HIDSAHLyNNEEQVGLAIR	Y8-M	359806998; 359806990; 24497583; 5453543
annexin A2	2	AyTNFDAER	Y2-D	209862831; 50845386; 50845388
annexin A2	23	AyTNFDAERDALNIETAIK	Y2-D	209862831; 50845386; 50845388
ATP synthase subunit beta, mitochondrial	3	AIAELGIyPAVDPLDSTSR	Y8-D	32189394
cofilin (1 and 2)	2	YALYDAtYETK	T7-D	5031635; 343887344; 33946278
cofilin (1 and 2)	3	YALyDATYETK	Y4-D	5031635; 343887344; 33946278
enolase (alpha)	6	AAVPSGASTGIyEALELRDNDKTR	Y12-D	4503571
enolase (alpha)	10	yISPDQLADLYK	Y1-D	319996655; 4503571
enolase (alpha)	4	yISPDQLADLyK	Y1-D; Y11-D	319996655; 4503571
enolase (alpha)	6	YISPDQLADLyK	Y11-D	319996655; 4503571
enolase (alpha, beta, and gamma)	36	AAVPSGASTGIyEALELR	Y12-D	5803011; 301897477; 301897469; 4503571; 301897479
exportin-2	2	mELSDANLQTLTEyLKK	Y14-D	29029559
glutathione S-transferase A5	3	NDGsLLFQQVPMVEIDGMK	S4-M	24308514
heat shock 70 kDa protein (1A/1B and 6)	4	IINEPTAAAIAyGLDR	Y12-D	194248072; 167466173; 34419635
heterogeneous nuclear ribonucleoprotein K	2	GsYGDLGGPIITTQVTIPK	S2-D	14165435; 14165439
heterogeneous nuclear ribonucleoprotein K	2	GSyGDLGGPIITTQVTIPK	Y3-D	14165435; 14165439
histone H4	2	TVTAMDVVyALK	Y9-D	28173560; 4504301
histone H4	6	TVTAMDVVyALKR	Y9-D	28173560; 4504301
histone H4	9	VFLENVIRDAVTyTEHAK	Y13-D	28173560; 4504301
malate dehydrogenase, mitochondrial	3	LtLYDIAHTPGVAADLSHIETK	T2-D	21735621
malate dehydrogenase, mitochondrial	5	LTLYDIAHtPGVAADLSHIETK	T9-D	21735621
malate dehydrogenase, mitochondrial	7	LTLyDIAHTPGVAADLSHIETK	Y4-D	21735621
nicotinamide phosphoribosyltransferase	16	TPAGNFVTLEEGKGDLEEyGQDLLHTVFK	Y19-D	5031977
nucleolin	3	NLPyKVTQDELKEVFEDAAEIR	Y4-D	55956788
peptidyl-prolyl cis−trans isomerase A	11	sIYGEKFEDENFILK	S1-D	10863927
peptidyl-prolyl cis−trans isomerase A	11	SIyGEKFEDENFILK	Y3-D	10863927
phosphoglycerate kinase (1 and 2)	2	LGDVyVNDAFGTAHR	Y5-D	31543397; 4505763
phosphoglycerate kinase 1	2	SVVLMSHLGRPDGVPMPDKySLEPVAVELK	Y20-D	4505763
pyruvate kinase isozymes M1/M2	6	TATESFASDPILyRPVAVALDTKGPEIR	Y13-D	332164775; 33286422; 33286418; 332164781; 332164779
small nuclear ribonucleoprotein Sm D1	2	yFILPDSLPLDTLLVDVEPK	Y1-D	5902102
transketolase	26	NMAEQIIQEIySQIQSK	Y11-D	205277463; 4507521; 384475521
triosephosphate isomerase	4	IAVAAQNcyK	Y9-D	226529917; 4507645

dx.doi.org/10.1021/pr500076t | J. Proteome Res. 2014, 13, 3583−3595

Table 2. continued

protein	PSM[a]	peptide sequence	adduct[b]	protein accession numbers[c]
triosephosphate isomerase	3	IIyGGSVTGATcK	Y3-D	226529917; 4507645
tubulin alpha chain	2	IHFPLATyAPVISAEK	Y8-D	57013276; 17921993; 156564363; 17921989; 393715091; 17986283; 46409270; 14389309
tubulin alpha chain	3	QLFHPEQLITGKEDAANNyAR	Y19-D	57013276; 17921993; 156564363; 17921989; 393715091; 17986283; 9507215; 301171345; 14389309
tubulin beta chain	10	GHyTEGAELVDSVLDVVR	Y3-D	29788768; 4507729; 29788785; 308235963; 5174735; 50592996
tubulin beta chain	27	GHyTEGAELVDSVLDVVRK	Y3-D	29788768; 4507729; 29788785; 308235963; 5174735; 50592996
tubulin beta chain	5	GHyTEGAELVDSVLDVVRK	Y3-M	29788768; 4507729; 29788785; 308235963; 5174735; 50592996
tubulin beta chain	8	ISVyYNEATGGK	Y4-D	29788785
tubulin beta chain	6	ISVYyNEATGGK	Y5-D	29788785
tubulin beta chain	3	yLTVAAVFR	Y1-D	29788785; 21361322; 5174735
tubulin beta-4B chain	3	INVYyNEATGGK	Y5-D	5174735

[a]Number peptide spectrum matches. Only PSM with an FDR ≤ 0.01 are included. [b]Adduct site by amino acid and location in peptide; D: dimethylphosphate and M: methylphosphate. [c]Accession number of all proteins sharing the peptide sequence.

tions. Two peptides containing this residue, one with a missed cleavage at the penultimate lysine, (LEKPAKYDDIK and LEKPAKYDDIKK), were identified. Both the dimethyl- and methyl-phosphate variants of the adduct were identified on this residue. For the LISWYDNEFGYSNR peptide, the dimethyl-phosphate adduct was found on residues 3, 5, and 11 (S312, Y314, and Y320), while the methylphosphate was found only on residue 11. Of particular interest is that residue 3 is a serine, making this one of the few nontyrosine adduct sites that was identified. The LDH analysis had the lowest coverage (55%), and we did not find any DDVP adducts on it.

Because of GAPDH's crucial role in the glycolysis/gluconeogenesis pathway and its susceptibility to DDVP at subcytotoxic concentrations (data not shown), we further examined GAPDH by incubating it with DDVP at two concentrations (50 and 500 μM). Interestingly, at these concentrations, we only found a DDVP adduct on the LEKPAKYDDIKK peptide at Y7. While this analysis was clearly not quantitative, it does hint at differing association constants for different adduct sites within a protein. It also confirms the accuracy of the theory behind the FP-biotin pull-down assay and confirms that the identified list of proteins (Table 1) contains putative targets of DDVP.

DDVP-Altered Enzymatic Activity of GAPDH

To assess the effects that DDVP adducts have on protein activity, we determined the enzymatic activity of representative target proteins (LDH and GAPDH) in DDVP-treated HepaRG cells and for DDVP-treated purified proteins. As shown in Figure 4, DDVP treatment for 4 h significantly reduced the enzymatic activity of GAPDH as a purified protein incubated with DDVP and also in HepaRG treated with different concentrations of DDVP. The inhibitory effects appear to be concentration-dependent, and DDVP rendered significant inhibitory effects at concentrations $\geq$ 500 μM ($p < 0.05$). The effects on LDH appear to be more limited. There was a trend in the purified protein data toward a reduction in activity, but at the highest concentration tested, the difference failed to reach significance ($p = 0.07$). Taken with the failure to identify an adduct on LDH, these findings suggest that DDVP is likely to have a low affinity for LDH. Nevertheless, the results provided a direct relation between DDVP interaction with GAPDH and enzymatic activity.

Pathways Affected by DDVP

To obtain a better understanding of DDVP toxicity in the liver, we performed a quantitative, label-free LC−MS analysis of proteins changing in abundance in HepaRG cells treated with 500 μM DDVP for 4 or 24 h (Supplemental Table 2 in the Supporting Information). Three biological replicates were performed. DDVP treatment induced changes in abundance of 49 proteins with at least one peptide changing by 1.5 fold (FDR <0.05) and average change for all identified peptides of at least 1.5 fold. Of the 16 proteins with abundance changes greater than 1.5 fold at both time points, the direction of change in abundance for 14 of the proteins was different after 4 h than after 24 h of treatment. In all cases but one, the abundance of the proteins was increased at 4 h and reduced at 24. It is unclear why the abundance of the majority of the differentially regulated proteins is declining at the later time point, although it may signal a shift from an anti-apoptotic to a pro-apoptotic state within the cell (see later).

To gain an understanding of the biological relationships between proteins changing in abundance from HepaRG cells

dx.doi.org/10.1021/pr5000076 | J. Proteome Res. 2014, 13, 3583−3595

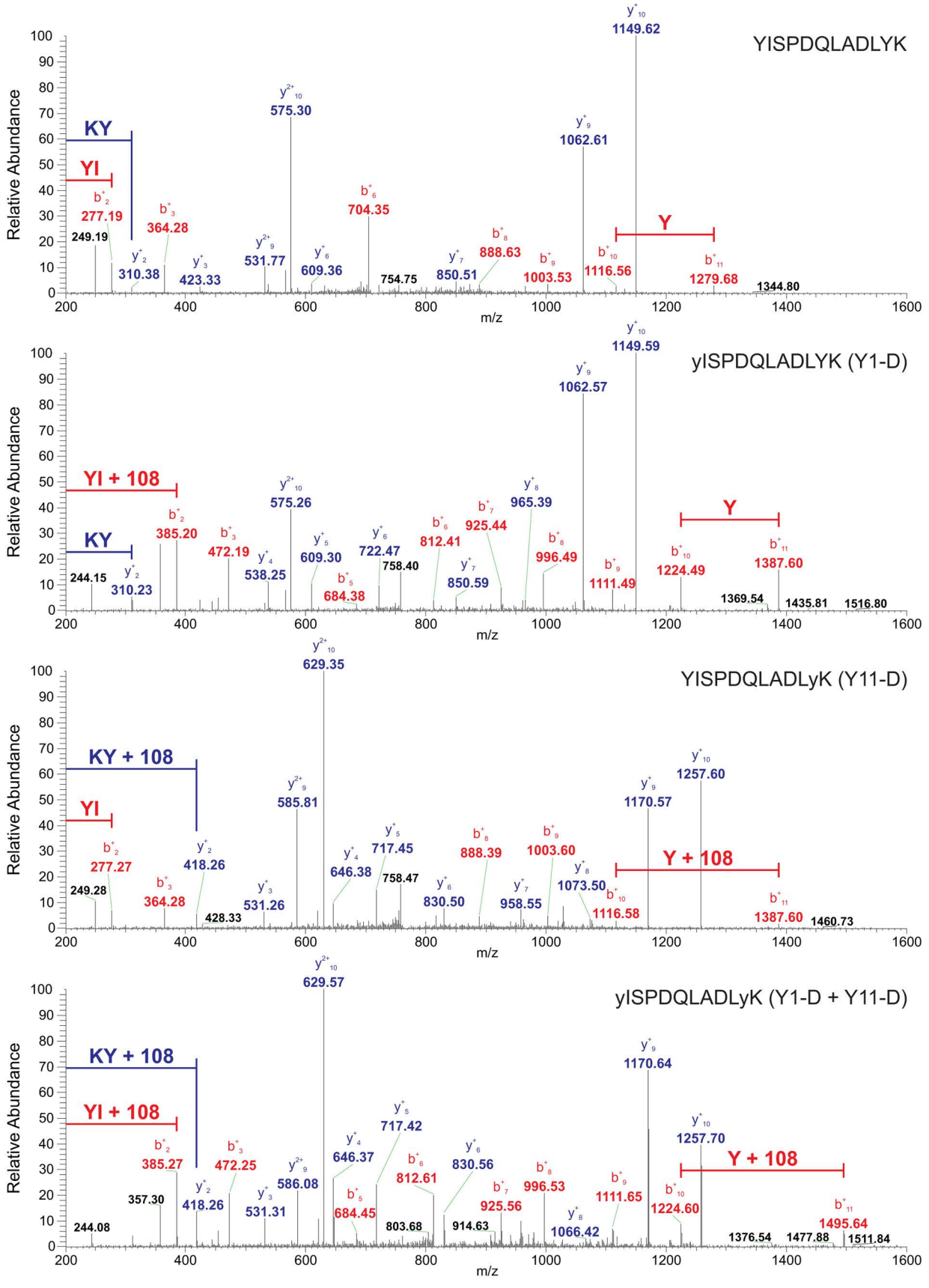

Figure 2. MS/MS spectra of an enolase peptide YISPDQLADLYK showing an increased mass of 108 Da indicating the presence of a dimethylphosphate (D) adduct on the first, penultimate, or both tyrosine residues. B ion series have been labeled in red and y ion series have been labeled in blue. CID fragmentation was used.

dx.doi.org/10.1021/pr5000076 | J. Proteome Res. 2014, 13, 3583−3595

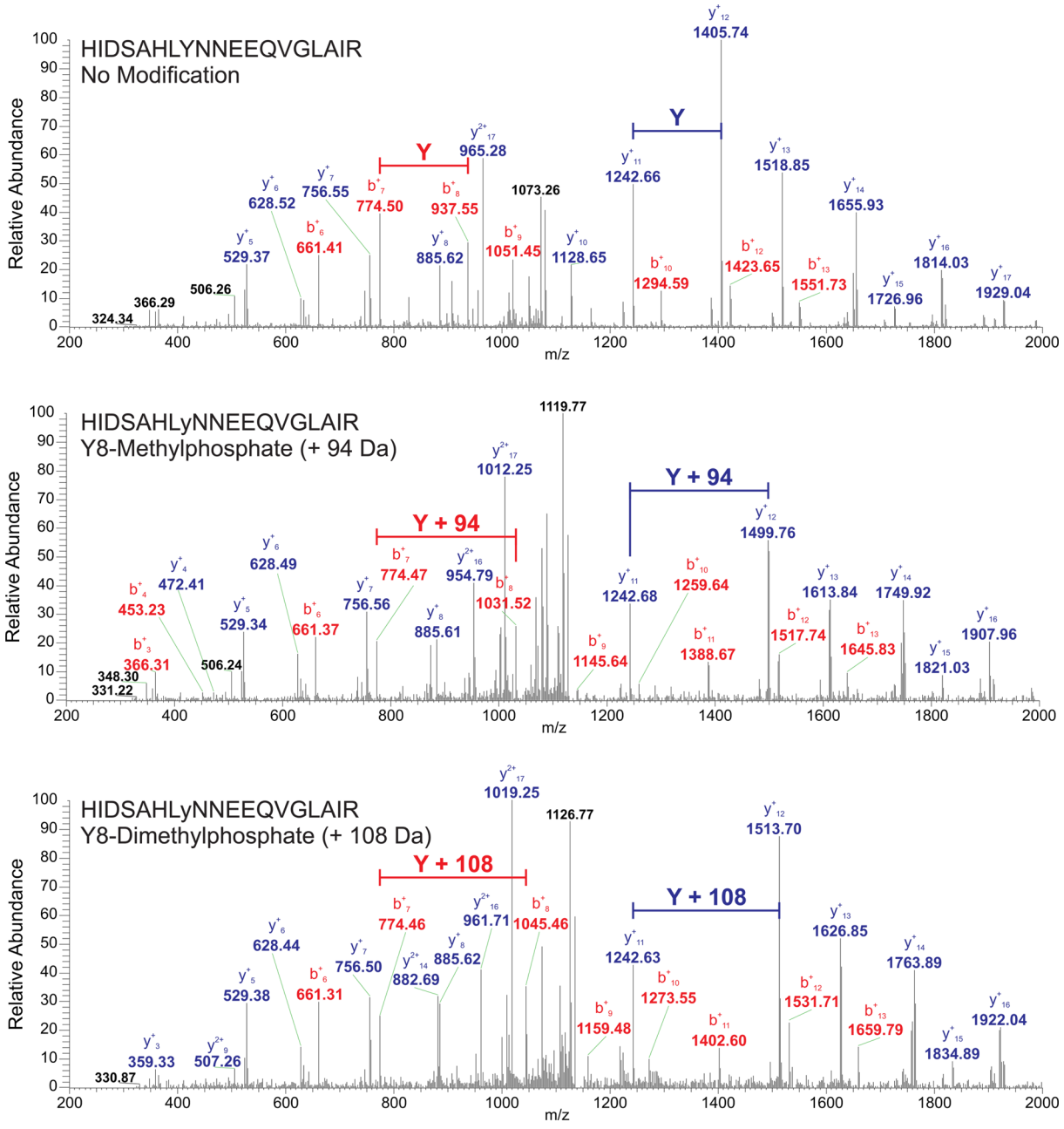

Figure 3. MS/MS spectra of an aldo-keto reductase peptide HIDSAHLYNNEEQVGLAIR showing a mass shift of 94 Da for the aged (methylphosphate) or of 108 Da for the unaged (dimethylphosphate) adducts found on the tyrosine residue at position 8. B ion series have been labeled in red and y ion series have been labeled in blue. CID fragmentation was used.

treated with DDVP (Supplemental Table 2 in the Supporting Information) and DDVP targets identified by FP-biotin or direct MS/MS (Tables 1 and 2), we combined the three lists, and a pathway analysis was performed using MetaCore. The analysis revealed 27 MetaCore maps of interest that have a minimum of two proteins from the list and at least one DDVP target identified by FP-biotin or MS/MS (Table 4). These pathways can be grouped into six categories, demonstrating the global effects of DDVP treatments. DDVP treatment can affect multiple biological processes critical to cell apoptosis and survival, remodeling, differentiation, energy regulation, stress response, and transport.

DDVP-induced cell death has been demonstrated in at least two studies using rat hepatocytes[39] or a porcine kidney epithelial cell line.[10] In the present study, DDVP-induced apoptosis after prolonged exposure is supported by proteomic data. For example, 14-3-3 proteins have been shown to be antiapoptotic.[40,41] DDVP adducts were identified on two 14-3-3 proteins (gamma and zeta/delta), and after 4 h of DDVP treatment, the 14-3-3 protein epsilon was increased in abundance by 1.9 fold and was available to block apoptosis. However, after 24 h of DDVP treatment, the abundance is below control levels (−1.4 fold). The change in abundance of this 14-3-3 proteins is likely to affect the dynamic regulation of key apoptotic proteins such as BAD, BIM, and BAX,[41] thus shifting the environment toward pro-apoptosis.

Pathway analysis also revealed that 11 Metacore maps involved in cell adhesion and remodeling may be affected by DDVP treatment (Table 4). DDVP formed adducts on several cytoskeletal proteins, including actin, tubulin, and cofilin. At 4 h

dx.doi.org/10.1021/pr5000076 | J. Proteome Res. 2014, 13, 3583−3595

Table 3. Adduct Sites Identified by LC−MS/MS on GAPDH after Incubation with 5 mM DDVP for 2 h

protein	PSM[a]	sequence	adduct[b]
glyceraldehyde-3-phosphate dehydrogenase	4	LEKPAKyDDIK	Y7-D
glyceraldehyde-3-phosphate dehydrogenase	2	LEKPAKyDDIK	Y7-M
glyceraldehyde-3-phosphate dehydrogenase	4	LEKPAKyDDIKK	Y7-D
glyceraldehyde-3-phosphate dehydrogenase	4	LEKPAKyDDIKK	Y7-M
glyceraldehyde-3-phosphate dehydrogenase	3	LIsWYDNEFGYSNR	S3-D
glyceraldehyde-3-phosphate dehydrogenase	4	LISWYDNEFGySNR	Y11-D
glyceraldehyde-3-phosphate dehydrogenase	10	LISWyDNEFGYSNR	Y5-D
glyceraldehyde-3-phosphate dehydrogenase	7	LISWyDNEFGYSNR	Y5-M

[a]Number of peptide spectrum matches. Only PSMs with an FDR ≤ 0.01 are included. [b]Adduct site by amino acid and location in peptide; D: dimethylphosphate and M: methylphosphate.

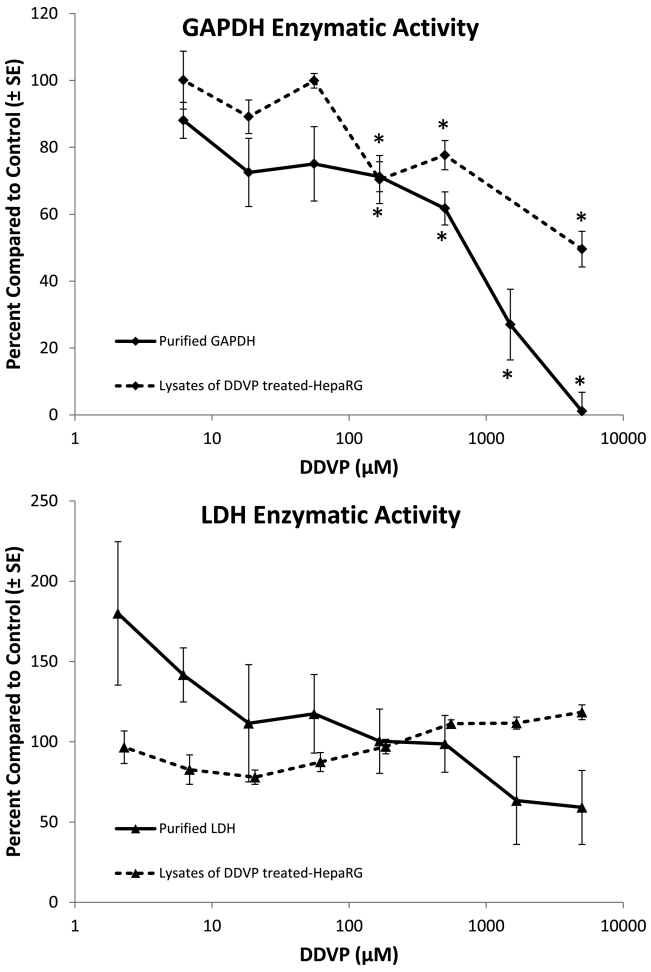

Figure 4. Enzymatic activity of GAPDH and LDH after exposure to DDVP. The GAPDH and LDH enzymatic activity of DDVP-treated HepaRG lysates, purified GAPDH, and purified LDH was measured after incubation with various concentrations of DDVP for 2 h. Untreated cells or enzymes were used as controls. Water was used as blank for kinetic studies (n = 4).

into the treatment, there was an increase in the abundance of cytoskeletal proteins such as actin and tubulins, suggesting that the cells still actively responded to physiological changes caused by DDVP. However, at 24 h, cytoskeletal processes appeared to be compromised. Specifically, DDVP caused a reduction in the abundance of the cytoskeletal structural proteins actin and tubulin and other regulators of actin conformation (e.g., spectrin and profilin). The effects of DDVP on cytoskeleton components overlapped with cell differentiation processes, including cell cycle regulation, epithelial to mesenchymal transition (EMT) process, and transport.

Previous studies, including ours (manuscript in preparation), suggest that DDVP treatment affects glucose homeostasis in multiple ways.[12,42−45] Here we found DDVP adduction to proteins crucial to the glycolytic/gluconeogenesis pathway such as phosphoglycerate kinase 1 (PGK1), triosephosphate isomerase (TPI1), glyceraldehyde-3 phosphate dehydrogenase (GAPDH), enolase (ENO), and malate dehydrogenase (MDH2). The results provide multiple points in which DDVP may interfere with glucose metabolism. Collectively, the current approach not only allows us to discover novel molecular mechanisms underlying DDVP toxicity but also provides additional molecular evidence supporting previous observations.

■ CONCLUSIONS

In the present study, we have demonstrated the usefulness of cell lysates to identify proteins modified by DDVP. We showed that DDVP-adduct formation and DDVP treatment altered enzymatic activity of at least one of these proteins (GAPDH). The DDVP modification sites we identified match a previously proposed OP-binding motif at tyrosines.[28] However, in addition to the modification at tyrosine residues, we also observed, although less frequently, DDVP binding at threonine and serine residues.

We found that DDVP-modified GAPDH, a well-known glycolytic enzyme, at one serine residue (S312) and three tyrosine residues (Y255, Y314, and Y320). Y314 is among a number of active-site amino acids that are directly involved in binding the NAD+ nicotinamide moiety to GAPDH and are responsible for catalytic activity.[46] Interestingly, DDVP was only found to form an adduct to this site at the highest concentration we tested (5 mM). At this concentration, GAPDH enzymatic activity was reduced to <10% of control. This high concentration may be necessary because of the inaccessibility of the tyrosine in the active site cleft. In contrast, DDVP modification at Y255, a known site that is required for GAPDH intranuclear accumulation and nuclear export,[47] occurred at all three tested concentrations (50, 500, and 5000 μM), consistent with a location on the surface of the protein.

In addition to its main role in the glycolytic pathway, GAPDH has recently emerged as a regulatory protein, controlling transcription, possessing kinase/phosphotransferase activity, catalyzing microtubule formation and polymerization, facilitating vesicular transport, regulating Ca^{2+} flux, modulating stress response molecules (i.e., glutathione, nitric oxide, and p53), and facilitating apoptosis.[46] Modification of GAPDH has been shown to induce instability of the tetrameric protein and affect enzyme activity.[48] The modification of GAPDH at a concentration as low as 50 μM may play into the induction of apoptosis by DDVP.[10,39] DDVP modification at Y255 may alter tetrameric GAPDH structure and interfere with GAPDH trafficking between the nucleus and cytoplasm, resulting in

dx.doi.org/10.1021/pr5000076 | J. Proteome Res. 2014, 13, 3583−3595

Table 4. Biological Pathways Containing Proteins Affected by DDVP Treatment

category	Metacore map	no. DDVP target proteins[a]
apoptosis and survival	Apoptosis and survival_Granzyme B signaling	4
apoptosis and survival	Development_IGF-1 receptor signaling	2
cell adhesion and remodeling	Cell adhesion_Gap junctions	5
cell adhesion and remodeling	Development_Slit-Robo signaling	5
cell adhesion and remodeling	Cytoskeleton remodeling_Regulation of actin cytoskeleton by Rho GTPases	4
cell adhesion and remodeling	Cell adhesion_Histamine H1 receptor signaling in the interruption of cell barrier integrity	3
cell adhesion and remodeling	Cell adhesion_Integrin-mediated cell adhesion and migration	3
cell adhesion and remodeling	Cytoskeleton remodeling_Cytoskeleton remodeling	3
cell adhesion and remodeling	Cytoskeleton remodeling_TGF, WNT and cytoskeletal remodeling	3
cell adhesion and remodeling	Cell adhesion_Alpha-4 integrins in cell migration and adhesion	2
cell adhesion and remodeling	Cell adhesion_Chemokines and adhesion	2
cell adhesion and remodeling	Cytoskeleton remodeling_Fibronectin-binding integrins in cell motility	2
cell adhesion and remodeling	Cytoskeleton remodeling_Role of PKA in cytoskeleton reorganization	2
cell differentiation	Cell cycle_Spindle assembly and chromosome separation	7
cell differentiation	Cell cycle_Role of Nek in cell cycle regulation	5
cell differentiation	Cytoskeleton remodeling_Reverse signaling by ephrin B	5
cell differentiation	Cell cycle_rRole of 14-3-3 proteins in cell cycle regulation	2
cell differentiation	Development_TGF-beta-dependent induction of EMT via RhoA, PI3K and ILK.	2
energy regulation	Glycolysis and gluconeogenesis (short map)	3
energy regulation	Glycolysis and gluconeogenesis p. 2	2
energy regulation	Pentose phosphate pathway	2
energy regulation	Transcription_Role of Akt in hypoxia induced HIF1 activation	2
energy regulation	Triacylglycerol metabolism p.1	2
stress response	Oxidative stress_Role of ASK1 under oxidative stress	2
transport	Transport_Macropinocytosis regulation by growth factors	6
transport	Cholesterol and Sphingolipids transport/Transport from Golgi and ER to the apical membrane (normal and CF)	1
transport	Transport_Intracellular cholesterol transport in norm	1

[a]Number of proteins predicted with DDVP adducts.

GAPDH accumulation in the nucleus, an event that is known to precede the onset of apoptosis.[49,50] Indeed, previous work has shown that alteration of the sequence in which Y255 is found resulted in intranuclear accumulation of GAPDH.[47]

Interestingly, the increased number of modifications at different residues in a concentration-dependent manner suggests that DDVP adduct formation may be promiscuous at high concentrations. Calculations based on the number of peptides identified with adducts versus the total number of peptides identified and the average MS/MS coverage of the proteins in the analysis (data not shown) suggest that many more proteins were likely to have DDVP adducts than were actually identified in this work. The average number of adducts might have approached one adduct per protein. Although DDVP appears to be highly reactive with polypeptides in general, in our lysates and cell culture experiments it displayed considerable specificity for tyrosines in the vicinity of positively charged arginines or lysines, as was previously observed with purified proteins.[16,20−22] We also found amino acids with a hydroxyl group within a few amino acids of the majority of the modified residues. On the basis of these characteristics, there appears to be a preference toward charged (most likely on the surface) regions of the protein, but we were unable to discern any additional characteristics that would help to determine specificity. Although the biological roles of the adducted sites are not likely to be a factor in predicting where DDVP will form a bond, many modifications were found at known phosphorylation sites, active proton donor sites, glutathione binding sites, or metal binding sites. Such sites are often on the surface of proteins, where they are accessible or are highly polar, which we predict would favor the DDVP reaction.

Using whole cell lysates, we captured a larger population of DDVP targets. However, most of these proteins appear to be abundant cellular constituents. Like others,[16,17,19,20] we did not find direct evidence of peptide modification by DDVP in exposed cells (data not shown). Explanations for our failure to detect covalent binding of DDVP to proteins in treated cells may be attributed to the low abundance of modified peptides due to the rapid metabolism of DDVP,[7−9] restricted exposure to DDVP because of intracellular compartmentalization, or poor ionization of the modified peptides. Alternatively, in vivo modification may not be the principal reason for alterations in cellular physiology following DDVP exposure. However, it is clear from this work and from the know inhibition of AChE

dx.doi.org/10.1021/pr5000076 | J. Proteome Res. 2014, 13, 3583−3595

that DDVP forms adducts, and it is through these adducts that it can inhibit protein functions.

We identified targets using the FP-biotin pull-down method, which provided indirect proof of DDVP−protein interaction, and used additional strategies,[16,17,25] including in vitro exposure, to provide direct proof of covalent binding of DDVP to proteins. As a result, we confirmed novel DDVP targets and provide supporting evidence to previous studies.

On the basis of the DDVP targets identified in vitro and the high-content proteomics data generated from DDVP-treated HepaRG cells, we utilized pathway analysis to predict the physiological consequences of DDVP exposure and identified a number of fundamental biological processes affected by DDVP exposure. This approach allowed us to characterize the relationship between DDVP's targets and other affected proteins. For example, as a target of DDVP, actin's functions would be compromised not only in cell adhesion remodeling processes but also in cell differentiation and survival biological pathways. Finally, the current approach provides the foundation for future hypothesis driven studies to understand the underlying mechanism of toxicity of DDVP in non-neuronal tissues.

■ ASSOCIATED CONTENT

Supporting Information

Supplemental Table 1: Sample sets used in this manuscript. Supplemental Table 2: Proteins changing in abundance at 4 or 24 h in HepaRG cells exposed to 500 μM DDVP. This material is available free of charge via the Internet at http://pubs.acs.org.

■ AUTHOR INFORMATION

Corresponding Author

*Phone: 301 619 7209. Fax: 301 619 7606. E-mail: john.a.lewis1@us.army.mil.

Notes

The authors declare no competing financial interest.

■ ACKNOWLEDGMENTS

We thank Alan Rosencrance for quantitative analysis of dichlorvos stocks and media and the PRIDE team for assistance in uploading the mass spectral data. The research was supported by the Military Operational Medicine Research Program of the U.S. Army Medical Research and Materiel Command. Opinions, interpretations, conclusions, and recommendations are those of the authors and are not necessarily endorsed by the U.S. Army. Citations of commercial organizations or trade names in this report do not constitute an official Department of the Army endorsement or approval of the products or services of these organizations. This research was partially supported by an appointment to the Postgraduate Research Participation Program at the U.S. Army Center for Environmental Health Research administered by the Oak Ridge Institute for Science and Education through an interagency agreement between the U.S. Department of Energy and USAMRMC.

■ REFERENCES

(1) Binukumar, B. K.; Bal, A.; Kandimalla, R.; Sunkaria, A.; Gill, K. D. Mitochondrial energy metabolism impairment and liver dysfunction following chronic exposure to dichlorvos. *Toxicology* **2010**, *270* (2−3), 77−84.

(2) Eddleston, M.; Buckley, N. A.; Eyer, P.; Dawson, A. H. Management of acute organophosphorus pesticide poisoning. *Lancet* **2008**, *371* (9612), 597−607.

(3) Binukumar, B. K.; Gill, K. D. Cellular and molecular mechanisms of dichlorvos neurotoxicity: cholinergic, nonchlolinergic, cell signaling, gene expression and therapeutic aspects. *Indian J. Exp. Biol.* **2010**, *48* (7), 697−709.

(4) Montgomery, M. P.; Kamel, F.; Saldana, T. M.; Alavanja, M. C.; Sandler, D. P. Incident diabetes and pesticide exposure among licensed pesticide applicators: Agricultural Health Study, 1993−2003. *Am. J. Epidemiol.* **2008**, *167* (10), 1235−1246.

(5) Khan, A. A.; Coppock, R. W.; Schuler, M. M.; Lillie, L. E. Effects of dichlorvos on blood cholinesterase activities of cattle. *Am. J. Vet. Res.* **1990**, *51* (1), 79−82.

(6) Li, B.; Ricordel, I.; Schopfer, L. M.; Baud, F.; Megarbane, B.; Nachon, F.; Masson, P.; Lockridge, O. Detection of adduct on tyrosine 411 of albumin in humans poisoned by dichlorvos. *Toxicol. Sci.* **2010**, *116* (1), 23−31.

(7) Loeffler, J. E.; Potter, J. C.; Scordelis, S. L.; Hendrickson, H. R.; Huston, C. K.; Page, A. C. Long-term exposure of swine to a (14C)dichlorvos atmosphere. *J. Agric. Food Chem.* **1976**, *24* (2), 367−371.

(8) Page, A. C.; Loeffler, J. E.; Hendrickson, H. R.; Huston, C. K.; DeVries, D. M. Metabolic fate of dichlorvos in swine. *Arch. Toxikol.* **1972**, *30* (1), 19−27.

(9) Potter, J. C.; Loeffler, J. E.; Collins, R. D.; Young, R.; Page, A. C. Carbon-14 balance and residues of dichlorvos and its metabolites in pigs dosed with dichlorvos- 14 C. *J. Agric. Food Chem.* **1973**, *21* (2), 163−166.

(10) Li, S.; Ran, X. Q.; Xu, L.; Wang, J. F. microRNA and mRNA expression profiling analysis of dichlorvos cytotoxicity in porcine kidney epithelial PK15 cells. *DNA Cell Biol.* **2011**, *30* (12), 1073−1083.

(11) Abdollahi, M.; Donyavi, M.; Pournourmohammadi, S.; Saadat, M. Hyperglycemia associated with increased hepatic glycogen phosphorylase and phosphoenolpyruvate carboxykinase in rats following subchronic exposure to malathion. *Comp. Biochem. Physiol., Part C: Toxicol. Pharmacol.* **2004**, *137* (4), 343−347.

(12) Sarin, S.; Gill, K. D. Dichlorvos induced alterations in glucose homeostasis: possible implications on the state of neuronal function in rats. *Mol. Cell. Biochem.* **1999**, *199* (1−2), 87−92.

(13) Lim, L. O. *Dichlorvos (DDVP): Risk Characterization Document*; California Environmental Protection Agency: Sacramento, CA, 1996.

(14) Hutson, D. H.; Hoadley, E. C. The metabolism of (14 C-methyl)dichlorvos in the rat and the mouse. *Xenobiotica* **1972**, *2* (2), 107−116.

(15) Costa, L. G. Current issues in organophosphate toxicology. *Clin. Chim. Acta* **2006**, *366* (1−2), 1−13.

(16) Schopfer, L. M.; Grigoryan, H.; Li, B.; Nachon, F.; Masson, P.; Lockridge, O. Mass spectral characterization of organophosphate-labeled, tyrosine-containing peptides: characteristic mass fragments and a new binding motif for organophosphates. *J. Chromatogr., B* **2010**, *878* (17−18), 1297−1311.

(17) Grigoryan, H.; Li, B.; Anderson, E. K.; Xue, W.; Nachon, F.; Lockridge, O.; Schopfer, L. M. Covalent binding of the organophosphorus agent FP-biotin to tyrosine in eight proteins that have no active site serine. *Chem. Biol. Interact.* **2009**, *180* (3), 492−498.

(18) Kidd, D.; Liu, Y.; Cravatt, B. F. Profiling serine hydrolase activities in complex proteomes. *Biochemistry (Moscow)* **2001**, *40* (13), 4005−4015.

(19) Ding, S. J.; Carr, J.; Carlson, J. E.; Tong, L.; Xue, W.; Li, Y.; Schopfer, L. M.; Li, B.; Nachon, F.; Asojo, O.; Thompson, C. M.; Hinrichs, S. H.; Masson, P.; Lockridge, O. Five tyrosines and two serines in human albumin are labeled by the organophosphorus agent FP-biotin. *Chem. Res. Toxicol.* **2008**, *21* (9), 1787−1794.

(20) Li, B.; Schopfer, L. M.; Grigoryan, H.; Thompson, C. M.; Hinrichs, S. H.; Masson, P.; Lockridge, O. Tyrosines of human and mouse transferrin covalently labeled by organophosphorus agents: a

new motif for binding to proteins that have no active site serine. *Toxicol. Sci.* **2009**, *107* (1), 144−155.
(21) Li, B.; Schopfer, L. M.; Hinrichs, S. H.; Masson, P.; Lockridge, O. Matrix-assisted laser desorption/ionization time-of-flight mass spectrometry assay for organophosphorus toxicants bound to human albumin at Tyr411. *Anal. Biochem.* **2007**, *361* (2), 263−272.
(22) Tacal, O.; Lockridge, O. Methamidophos, dichlorvos, O-methoate and diazinon pesticides used in Turkey make a covalent bond with butyrylcholinesterase detected by mass spectrometry. *J. Appl. Toxicol.* **2010**, *30* (5), 469−475.
(23) Fleisher, J. H.; Harris, L. W. Dealkylation as a mechanism for aging of cholinesterase after poisoning with pinacolyl methylphosphonofluoridate. *Biochem. Pharmacol.* **1965**, *14* (5), 641−650.
(24) Vizcaíno, J. A.; Deutsch, E. W.; Wang, R.; Csordas, A.; Reisinger, F.; Ríos, D.; Dianes, J. A.; Sun, Z.; Farrah, T.; Bandeira, N.; Binz, P. A.; Xenarios, I.; Eisenacher, M.; Mayer, G.; Gatto, L.; Campos, A.; Chalkley, R. J.; Kraus, H. J.; Albar, J. P.; Martinez-Bartolomé, S.; Apweiler, R.; Omenn, G. S.; Martens, L.; Jones, A. R.; Hermjakob, H. ProteomeXchange provides globally co-ordinated proteomics data submission and dissemination. *Nature Biotechnol.* **2014**, *30* (3), 223−226.
(25) Grigoryan, H.; Li, B.; Xue, W.; Grigoryan, M.; Schopfer, L. M.; Lockridge, O. Mass spectral characterization of organophosphate-labeled lysine in peptides. *Anal. Biochem.* **2009**, *394* (1), 92−100.
(26) Peeples, E. S.; Schopfer, L. M.; Duysen, E. G.; Spaulding, R.; Voelker, T.; Thompson, C. M.; Lockridge, O. Albumin, a new biomarker of organophosphorus toxicant exposure, identified by mass spectrometry. *Toxicol. Sci.* **2005**, *83* (2), 303−312.
(27) Liu, Y.; Patricelli, M. P.; Cravatt, B. F. Activity-based protein profiling: the serine hydrolases. *Proc. Natl. Acad. Sci. U. S. A.* **1999**, *96* (26), 14694−14699.
(28) Lockridge, O.; Schopfer, L. M. Review of tyrosine and lysine as new motifs for organophosphate binding to proteins that have no active site serine. *Chem. Biol. Interact.* **2010**, *187* (1−3), 344−348.
(29) Mindnich, R. D.; Penning, T. M. Aldo-keto reductase (AKR) superfamily: genomics and annotation. *Hum. Genomics* **2009**, *3* (4), 362−370.
(30) Ji, Q.; Aoyama, C.; Nien, Y. D.; Liu, P. I.; Chen, P. K.; Chang, L.; Stanczyk, F. Z.; Stolz, A. Selective loss of AKR1C1 and AKR1C2 in breast cancer and their potential effect on progesterone signaling. *Cancer Res.* **2004**, *64* (20), 7610−7617.
(31) Wang, S.; Yang, Q.; Fung, K. M.; Lin, H. K. AKR1C2 and AKR1C3 mediated prostaglandin D2 metabolism augments the PI3K/Akt proliferative signaling pathway in human prostate cancer cells. *Mol. Cell. Endocrinol.* **2008**, *289* (1−2), 60−66.
(32) Kleinschmidt, A. M.; Martinson, H. G. Role of histone tyrosines in nucleosome formation and histone-histone interaction. *J. Biol. Chem.* **1984**, *259* (1), 497−503.
(33) Booth, E. D.; Jones, E.; Elliott, B. M. Review of the in vitro and in vivo genotoxicity of dichlorvos. *Regul. Toxicol. Pharmacol.* **2007**, *49* (3), 316−326.
(34) Bettaieb, A.; Bakke, J.; Nagata, N.; Matsuo, K.; Xi, Y.; Liu, S.; AbouBechara, D.; Melhem, R.; Stanhope, K.; Cummings, B.; Graham, J.; Bremer, A.; Zhang, S.; Lyssiotis, C. A.; Zhang, Z. Y.; Cantley, L. C.; Havel, P. J.; Haj, F. G. Protein tyrosine phosphatase 1B regulates pyruvate kinase M2 tyrosine phosphorylation. *J. Biol. Chem.* **2013**, *288* (24), 17360−17371.
(35) Lee, W. H.; Choi, J. S.; Byun, M. R.; Koo, K. T.; Shin, S.; Lee, S. K.; Surh, Y. J. Functional inactivation of triosephosphate isomerase through phosphorylation during etoposide-induced apoptosis in HeLa cells: potential role of Cdk2. *Toxicology* **2010**, *278* (2), 224−228.
(36) Jin, X.; Wang, L. S.; Xia, L.; Zheng, Y.; Meng, C.; Yu, Y.; Chen, G. Q.; Fang, N. Y. Hyper-phosphorylation of alpha-enolase in hypertrophied left ventricle of spontaneously hypertensive rat. *Biochem. Biophys. Res. Commun.* **2008**, *371* (4), 804−809.
(37) Cooper, J. A.; Esch, F. S.; Taylor, S. S.; Hunter, T. Phosphorylation sites in enolase and lactate dehydrogenase utilized by tyrosine protein kinases in vivo and in vitro. *J. Biol. Chem.* **1984**, *259* (12), 7835−7841.
(38) Grigoryan, H.; Schopfer, L. M.; Thompson, C. M.; Terry, A. V.; Masson, P.; Lockridge, O. Mass spectrometry identifies covalent binding of soman, sarin, chlorpyrifos oxon, diisopropyl fluorophosphate, and FP-biotin to tyrosines on tubulin: a potential mechanism of long term toxicity by organophosphorus agents. *Chem. Biol. Interact.* **2008**, *175* (1−3), 180−186.
(39) Yamano, T. Dissociation of DDVP-induced DNA strand breaks from oxidative damage in isolated rat hepatocytes. *Toxicology* **1996**, *108* (1−2), 49−56.
(40) Clapp, C.; Portt, L.; Khoury, C.; Sheibani, S.; Norman, G.; Ebner, P.; Eid, R.; Vali, H.; Mandato, C. A.; Madeo, F.; Greenwood, M. T. 14−3-3 protects against stress-induced apoptosis. *Cell Death Dis.* **2012**, *3*, e348.
(41) Morrison, D. K. The 14−3-3 proteins: integrators of diverse signaling cues that impact cell fate and cancer development. *Trends Cell Biol.* **2009**, *19* (1), 16−23.
(42) Romero-Navarro, G.; Lopez-Aceves, T.; Rojas-Ochoa, A.; Fernandez Mejia, C. Effect of dichlorvos on hepatic and pancreatic glucokinase activity and gene expression, and on insulin mRNA levels. *Life Sci.* **2006**, *78* (9), 1015−1020.
(43) Sarin, S.; Gill, K. D. Biochemical characterization of dichlorvos-induced delayed neurotoxicity in rat. *IUBMB Life* **2000**, *49* (2), 125−130.
(44) Verma, S. R.; Rani, S.; Tonk, I. P.; Dalela, R. C. Pesticide-induced dysfunction in carbohydrate metabolism in three freshwater fishes. *Environ. Res.* **1983**, *32* (1), 127−133.
(45) Sarin, S.; Gill, K. D. Biochemical and behavioral deficits in adult rat following chronic dichlorvos exposure. *Pharmacol., Biochem. Behav.* **1998**, *59* (4), 1081−1086.
(46) Butterfield, D. A.; Hardas, S. S.; Lange, M. L. Oxidatively modified glyceraldehyde-3-phosphate dehydrogenase (GAPDH) and Alzheimer's disease: many pathways to neurodegeneration. *J. Alzheimer's Dis.* **2010**, *20* (2), 369−393.
(47) Brown, V. M.; Krynetski, E. Y.; Krynetskaia, N. F.; Grieger, D.; Mukatira, S. T.; Murti, K. G.; Slaughter, C. A.; Park, H. W.; Evans, W. E. A novel CRM1-mediated nuclear export signal governs nuclear accumulation of glyceraldehyde-3-phosphate dehydrogenase following genotoxic stress. *J. Biol. Chem.* **2004**, *279* (7), 5984−5992.
(48) Ryzlak, M. T.; Pietruszko, R. Heterogeneity of glyceraldehyde-3-phosphate dehydrogenase from human brain. *Biochim. Biophys. Acta* **1988**, *954* (3), 309−324.
(49) Ishitani, R.; Sunaga, K.; Tanaka, M.; Aishita, H.; Chuang, D. M. Overexpression of glyceraldehyde-3-phosphate dehydrogenase is involved in low K+-induced apoptosis but not necrosis of cultured cerebellar granule cells. *Mol. Pharmacol.* **1997**, *51* (4), 542−550.
(50) Ishitani, R.; Tanaka, M.; Sunaga, K.; Katsube, N.; Chuang, D. M. Nuclear localization of overexpressed glyceraldehyde-3-phosphate dehydrogenase in cultured cerebellar neurons undergoing apoptosis. *Mol. Pharmacol.* **1998**, *53* (4), 701−707.

■ NOTE ADDED AFTER ASAP PUBLICATION

Figure 3 has been updated. The revised version was re-posted on August 1, 2014.